J|A|C|S
ARTICLES

Published on Web 06/04/2009

Probing Single-Molecule Interfacial Geminate Electron−Cation Recombination Dynamics

Yuanmin Wang, Xuefei Wang, and H. Peter Lu*

Bowling Green State University, Center for Photochemical Sciences, Department of Chemistry, Bowling Green, Ohio 43403

Received April 2, 2009; E-mail: hplu@bgsu.edu

Abstract: Interfacial electron−cation recombination in zinc-tetra (4-carboxyphenyl) porphyrin (ZnTCPP)/TiO_2 nanoparticle system has been probed at the single-molecule level by recording and analyzing photon-to-photon pair times of the ZnTCPP fluorescence. We have developed a novel approach to reveal the hidden single-molecule interfacial electron−cation recombination dynamics by analyzing the autocorrelation function and a proposed convoluted single-molecule interfacial electron−cation recombination model. Our results suggest that the fluctuations of the interfacial electron transfer (ET) reactivity modulate the ET cycles as well as the interfacial electron−cation recombination dynamics. On the basis of this model, the single-molecule electron−cation recombination time of ZnTCPP/TiO_2 system is deduced to be at time scale of 10^{-5} s. The autocorrelation of photon-to-photon pair times as well as the convoluted ET model has been further demonstrated by simulation and interpreted in terms of the interfacial ET reactivity fluctuation and blinking. Our approach not only can effectively probe the single-molecule interfacial electron−cation dynamics but also can be applied to other single-molecule ground-state regeneration dynamics occurring at interfaces and within condensed phases.

Introduction

Interfacial electron transfer (ET) plays a critical role in chemical and biological systems, such as catalysis, bioremediation, and solar energy conversion. Specifically, interfacial ET in TiO_2-based dye-sensitization systems is important to solar energy technology and photocatalysis.[1−4] There are two major electron transfer processes involved in the photoinduced electron transfer at a dye/semiconductor interface: forward electron transfer (FET)[5,6] from an excited state of a dye molecule to the conduction band or energetically accessible surface states of TiO_2 semiconductor and backward electron transfer (BET)[7,8] of the excess electron which recombines with the dye molecule's cation. The FET is typically ultrafast in the femtosecond to several hundred picosecond range.[4,7−15] Following the FET, the thermalized injected electron is localized to either the sub-band states or surface states of the TiO_2 semiconductor.[16−20] Typically, a BET from the semiconductor to the oxidated dye molecules will follow.[7,8,18,20−26] The complex BET dynamics is often nonexponential, ranging from subnanoseconds to several milliseconds,[7,8,14,18,22,24,26] probably because of the existence of trap states and non-Brownian diffusion motions of the electrons within the semiconductor. Designing an efficient solar energy harvesting system entails controlling the rate of the BET process in order to generate long-lived charge-separated states so that the excess electron can have a high probability of escaping from the BET pathway and can contribute to the buildup of photovoltaics. Characterization of the BET dynamics

(1) O'Regan, B.; Grätzel, M. *Nature* **1991**, *353*, 737–740.
(2) Kamat, P. V. *J. Phys. Chem. C* **2007**, *111*, 2834–2860.
(3) Robertson, N. *Angew. Chem., Int. Ed.* **2008**, *47*, 1012–1014.
(4) Biju, V.; Micic, M.; Hu, D.; Lu, H. P. *J. Am. Chem. Soc.* **2004**, *126*, 9374–9381.
(5) Anderson, N. A.; Lian, T. Q. *Annu. Rev. Phys. Chem.* **2005**, *56*, 491–519.
(6) Watson, D. F.; Meyer, G. J. *Annu. Rev. Phys. Chem.* **2005**, *56*, 119–156.
(7) Pan, J.; Benkö, G.; Xu, Y.; Pascher, T.; Sun, L.; Sundström, V.; Polivka, T. *J. Am. Chem. Soc.* **2002**, *124*, 13949–13957.
(8) Matylitsky, V. V.; Lenz, M. O.; Wachtveitl, J. *J. Phys. Chem. B* **2006**, *110*, 8372–8379.
(9) Kondov, I.; Čižek, M.; Benesch, C.; Wang, H. B.; Thoss, M. *J. Phys. Chem. C* **2007**, *111*, 11970–11981.
(10) Abuabara, S. G.; Rego, L. G.; Batista, V. S. *J. Am. Chem. Soc.* **2005**, *127*, 18234–18242.
(11) Kondov, I.; Thoss, M.; Wang, H. *J. Phys. Chem. A* **2006**, *110*, 1364–1374.
(12) Liu, F.; Meyer, G. J. *J. Am. Chem. Soc.* **2005**, *127*, 824–825.
(13) Ramakrishna, G.; Verma, S.; Jose, D. A.; Kumar, D. K.; Das, A.; Palit, D. K.; Ghosh, H. N. *J. Phys. Chem. B* **2006**, *110*, 9012–9021.
(14) She, C.; Guo, J.; Irle, S.; Morokuma, K.; Mohler, D. L.; Zabri, H.; Odobel, F.; Youm, K. T.; Liu, F.; Hupp, J. T.; Lian, T. *J. Phys. Chem. A* **2007**, *111*, 6832–6842.
(15) Ramakrishna, G.; Singh, A. K.; Palit, D. K.; Ghosh, H. N. *J. Phys. Chem. B* **2004**, *108*, 4775–4783.
(16) Fox, M. A.; Dulay, M. T. *Chem. Rev.* **1993**, *93*, 341–357.
(17) Asbury, J. B.; Hao, E.; Wang, Y. Q.; Ghosh, H. N.; Lian, T. Q. *J. Phys. Chem. B* **2001**, *105*, 4545–4557.
(18) Hao, E. C.; Anderson, N. A.; Asbury, J. B.; Lian, T. Q. *J. Phys. Chem. B* **2002**, *106*, 10191–10198.
(19) Ramakrishna, G.; Ghosh, H. N. *J. Phys. Chem. A* **2002**, *106*, 2545–2553.
(20) Durrant, J. R. *J. Photochem. Photobiol., A* **2002**, *148*, 5–10.
(21) Duonghong, D.; Ramsden, J.; Grätzel, M. *J. Am. Chem. Soc.* **1982**, *104*, 2977–2985.
(22) Ghosh, H. N. *J. Phys. Chem. B* **1999**, *103*, 10382–10387.
(23) Holman, M. W.; Liu, R. C.; Adams, D. M. *J. Am. Chem. Soc.* **2003**, *125*, 12649–12654.
(24) Huber, R.; Moser, J. E.; Grätzel, M.; Wachtveitl, J. *Chem. Phys.* **2002**, *285*, 39–45.
(25) Huang, S. Y.; Schlichthorl, G.; Nozik, A. J.; Grätzel, M.; Frank, A. J. *J. Phys. Chem. B* **1997**, *101*, 2576–2582.
(26) Liu, D.; Fessenden, R. W.; Hug, G. L.; Kamat, P. V. *J. Phys. Chem. B* **1997**, *101*, 2583–2590.

10.1021/ja902640q CCC: $40.75

is therefore important for an understanding of solar energy conversion within a solar cell and interfacial redox reactions. Conventional ensemble-averaged measurements often encounter various interferences from molecular aggregation, multiple electron injection to a single particle, and multiple electron−cation recombinations on the surface of a single particle. Single-molecule spectroscopy[27−32] is a powerful way of deciphering the inhomogeneous interfacial ET dynamics by studying one molecule on one TiO_2 nanoparticle involving both FET and BET of a single electron at a time. Single-molecule spectroscopy has been applied to study intramolecular[33,34] and interfacial ET dynamics,[4,23,35−39] and the interfacial ET dynamics were found to be intermittent because of ET reactivity fluctuations[4,36−38,40] associated with single-molecule fluorescence intensity blinking and fluctuations. Our single-molecule spectroscopy studies of single-molecule interfacial electron transfer dynamics are more focused on the fundamental understanding of the interfacial redox reactivity, which is related broadly to catalysis and surface chemistry, in addition to our interests on technically improving the solar energy conversion efficiency. In this paper, we report the single-molecule recombination dynamics of the zinc-tetra (4-carboxyphenyl) porphyrin (ZnTCPP)/TiO_2 nanoparticle system. At the single-molecule level, the electron−cation recombination dynamics is analyzed through a convoluted interfacial electron−cation recombination process, and the recombination time of ZnTCPP/TiO_2 system is deduced to be at $\sim 10^{-5}$ s time scale.

Experimental Section

ZnTCPP (Frontier Scientific), ethanol (Aldrich), dichloromethane (EMD chemicals), and poly(methylmethacrylate) (PMMA) (typical MW 15 000, Aldrich) were used as provided. TiO_2 nanoparticles were prepared using hydrolysis of the titanium isopropoxide as a precursor according to a typical literature method.[41] Samples for single-molecule experiments were prepared in a similar procedure that we have reported previously.[4] Twenty-five microliters of 0.1 nM ZnTCPP in ethanol solution was first spin-coated to a clean coverslip (Fisher, 18 mm × 18 mm) at 3000 rpm and was overlaid by spin-coating 50 μL PMMA (in CH_2Cl_2, 1 mg/mL) to form a thin film to protect the dye molecules from singlet O_2 photobleaching and quenching. For a control experiment, 50 μL of TiO_2 NP solution was first spin-coated on a coverslip and then was overlaid by ZnTCPP and a thin PMMA film.

The detailed description of our optical measurements has been published elsewhere.[4] Single-molecule fluorescence spectroscopy and imaging were recorded by Axiovert 135 inverted scanning confocal microscope equipped with a 100×, 1.3 NA oil immersion objective (Zeiss FLUAR) and a close-loop nanoscale-precision piezoelectric scanning stage to control the position of a sample. A continuous-wave (CW) laser (532 nm, CrystaLaser) was used to pump the sample at about 200 nW. A beam splitter, Z532rdc (Chroma), was used to reflect the excitation light into the objective. The emission light passed through the emission filter HQ545lp (Chroma) and was collected by a single-photon-counting avalanche photodiode (APD) detector (Perkin-Elmer SPCMAQR-14). Photostamping data was recorded by a time-correlated single-photon-counting (TCSPC) system (SPC-830, Becker & Hickl GmbH) in an FIFO (first-in first-out) mode.

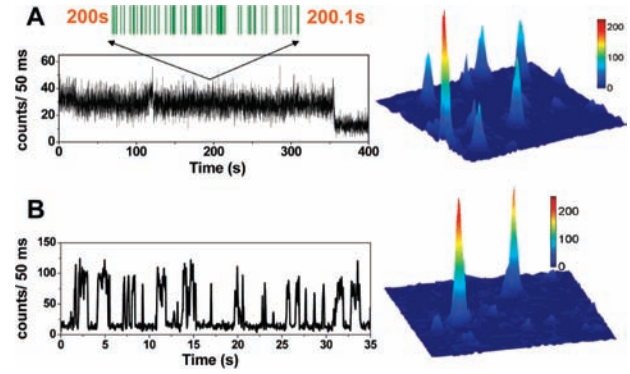

Figure 1. Fluorescence emission trajectory and optical imaging (10 μm × 10 μm) for a single ZnTCPP molecule on (A) a clean cover glass and (B) TiO_2 nanoparticle coated surface. In A, photostamping data from 200 to 200.1 s is displayed. Even under the same experimental condition, the measured photocounts in A (~40 counts/50 ms) is different from that of the bright state in B (~100 counts/50 ms). This is because the difference between the transition dipole direction of the ZnTCPP molecule and the laser polarization angle will contribute much to the measured photocounts.

Results and Discussion

ZnTCPP/TiO_2 interfacial electron transfer has been studied at the ensemble-averaged level extensively, being demonstrated as an efficient photosensitization system.[42−44] Figure 1 shows the fluorescence emission trajectories and optical images for single ZnTCPP molecules on a clean cover glass (Figure 1A) and on a TiO_2 nanoparticle covered surface (Figure 1B). The fluorescence trajectory from ZnTCPP/TiO_2 (Figure 1B) shows significant fluctuations and blinkings with dark times at sub-second to second time scales, whereas the single-molecule fluorescence of ZnTCPP on glass surface (without the possibility of interfacial ET) is essentially stable under the same experimental condition. It is an apparent paradox that single-molecule fluorescence is still observable along with interfacial electron transfer processes for ZnTCPP/TiO_2 dye-sensitized interfacial system. In our previous publication about ET in this and other similar systems,[4,37] we demonstrated that single dye molecules involve electron transfer activity intermittency reflected by single-molecule fluorescence blinking or fluctuations. When the interfacial ET reactivity is high, the ultrafast redox reactions dictate the fate of the singlet excited state of the dye molecules, and the fluorescence quantum efficiency is low or close to zero. In contrast, when the redox reactivity is low or nonexistent, the fluorescence quantum efficiency is high and the fluorescence

(27) Betzig, E.; Chichester, R. J. *Science* **1993**, *262*, 1422–1425.
(28) Trautman, J. K.; Macklin, J. J.; Brus, L. E.; Betzig, E. *Nature* **1994**, *369*, 40–42.
(29) Xie, X. S.; Dunn, R. C. *Science* **1994**, *265*, 361–364.
(30) VandenBout, D. A.; Yip, W. T.; Hu, D. H.; Fu, D. K.; Swager, T. M.; Barbara, P. F. *Science* **1997**, *277*, 1074–1077.
(31) Macklin, J. J.; Trautman, J. K.; Harris, T. D.; Brus, L. E. *Science* **1996**, *272*, 255–258.
(32) Lu, H. P.; Xie, X. S. *Nature* **1997**, *385*, 143–146.
(33) Liu, R. C.; Holman, M. W.; Zang, L.; Adams, D. M. *J. Phys. Chem. A* **2003**, *107*, 6522–6526.
(34) Hu, D. H.; Lu, H. P. *J. Phys. Chem. B* **2005**, *109*, 9861–9864.
(35) Lu, H. P.; Xie, X. S. *J. Phys. Chem. B* **1997**, *101*, 2753–2757.
(36) Cui, S. C.; Tachikawa, T.; Fujitsuka, M.; Majima, T. *J. Phys. Chem. C* **2008**, *112*, 19625–19634.
(37) Wang, Y.; Wang, X.; Ghosh, S. K.; Lu, H. P. *J. Am. Chem. Soc.* **2009**, *131*, 1479–1487.
(38) Issac, A.; Jin, S.; Lian, T. *J. Am. Chem. Soc.* **2008**, *130*, 11280–11281.
(39) Leite, V. B. P.; Alonso, L. C. P.; Newton, M.; Wang, J. *Phys. Rev. Lett.* **2005**, *95,* 118301 (1−4).
(40) Wang, J.; Wolynes, P. *Phys. Rev. Lett.* **1995**, *74*, 4317–4320.
(41) Duonghong, D.; Borgarello, E.; Grätzel, M. *J. Am. Chem. Soc.* **1981**, *103*, 4685–4690.
(42) Kalyanasundaram, K.; Vlachopoulos, N.; Krishnan, V.; Monnier, A.; Grätzel, M. *J. Phys. Chem.* **1987**, *91*, 2342–2347.
(43) Savenije, T. J.; Goossens, A. *Phys. Rev. B* **2001**, *64,* 115323 (1−9).
(44) Cherian, S.; Wamser, C. C. *J. Phys. Chem. B* **2000**, *104*, 3624–3629.

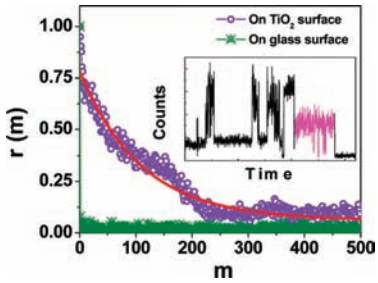

Figure 2. Normalized autocorrelation functions ($r(m)$) of pair times for a single molecule on clean cover glass (in "green", calculated from Figure 1A) and TiO_2 surfaces (in "purple", calculated from the colored state of the inserted trajectory; binning time: 100 ms).

intensity is high.[4,37] In our previous publications, we also reported a series of control experiments to demonstrate that the single-molecule fluorescence blinking is not due to (1) rare and slow (millisecond to subsecond) interfacial electron transfer events, (2) dye molecule triplet state blinking, or (3) molecular transition dipole rotations. We have conducted similar control experiments for the ZnTCPP/TiO_2 nanoparticle system and have reached the same conclusion.[37] Although it is beyond the scope of this paper, we have reported Raman spectroscopy studies on the molecular dye−TiO_2 vibrational coupling origin of the intermittent interfacial electron transfer dynamics in a dye-sensitized TiO_2 nanoparticle system.[45] We previously demonstrated a single-molecule photon antibunching analysis of intramolecular backward metal-to-ligand charge-transfer (MLCT) dynamics.[34] Here, we focus our discussion on probing the dynamics of interfacial BET process, that is, electron−cation ($ZnTCPP^+$) recombination process, for ZnTCPP/TiO_2 nanoparticle system.

Single-molecule photostamping spectroscopy records arrival time, delay time from excitation, and time sequence of every detected emission photon from a single molecule. Therefore, the photon-to-adjacent-photon pair time can be precisely recorded (as shown in Figure 1A). In a single-molecule photon-stamping measurement, each photon detected is emitted from the S_1 excited state of a dye molecule, and the same molecule will not be able to emit another photon until the dye molecule returns back to the ground state, S_0. In the excited state, a dye molecule will not emit a photon through an $S_1 \rightarrow S_0$ radiative transition if the molecule involves an ultrafast FET process reaching a charge-separation state of a dye cation and an excess electron in TiO_2. The cation is mostly nonfluorescent, and the dye molecule can only emit another photon when a BET occurs reducing the cation back to a neutral ground state, S_0. Therefore, statistical analysis of the relationship between adjacent photon-to-photon pair times can be a specific way to probe the interfacial ET dynamics. Autocorrelation function calculation is a typical approach to analyze fluctuation dynamics. Considering BET time is the main contribution to the photon-to-photon pair time since the rate of FET is typically 10^3-10^6 times faster than the time of BET in an excitation event of ZnTCPP/TiO_2, it is possible to probe BET dynamics by analyzing the correlation of single-molecule pair-time time trajectories. Figure 2 shows the normalized autocorrelation function of a pair-time trajectory calculated from a photon arrival time trajectory. The autocorrelation function is calculated by

$$r(m) = \left[n\sum_i^n t_i t_{i+m} - \left(\sum_i^n t_i\right)^2\right] \Big/ \left[n\sum_i^n t_i^2 - \left(\sum_i^n t_i\right)^2\right]$$

where i and m are the index numbers of a photon in a detected photon arrival time trajectory of total n photons, t_i is the pair time between a pair of photons i and $i + 1$, and t_{i+m} is the pair time between a pair of photons i and $i + m$; m varies from i to n.[46] For the sample of ZnTCPP on glass, the autocorrelation result shows zero amplitude at indexes larger than zero and a spike at index zero because of measurement noise and the fast fluctuations beyond measurement time resolution (Figure 2). There is no correlation between the pair times when there is no interfacial electron transfer occurrence, which is consistent with the stochastic nature of the fluorescence cycles under CW laser excitation. Remarkably, for ZnTCPP/TiO_2, the pair time of a state (color-highlighted part in the trajectory, Figure 2, inset) with relatively higher ET activity gives a well-defined correlation function. The correlation function suggests that there is a correlation in the photon-to-photon pair times and that the correlation decays exponentially with decay parameter of $m = 110 \pm 10$. Considering the average pair time for this state to be 0.65 ms, we calculate that the correlation time is about 72 ± 7 ms. The correlation disappears when the pair times are separated by 250 index numbers or more (Figure 2).

The correlation of photon-to-photon pair times in interfacial electron−cation recombination dynamics (Figure 3) is averaged-out in ensemble-averaged measurements and can only be revealed in a single-molecule measurement. Photogeneration of free carriers in low-mobility material heterojunctions[47,48] has been analyzed by the geminate recombination theory of Onsager[49] and Braun.[50] Marsh et al.[51] have demonstrated that the geminate recombination is the dominant loss mechanism for photon-excited charge separations in organic or hybrid solar cells. Photocurrent generation depends on the competition between dissociation and recombination of geminate electron−cation pairs. The electron drift mobility in nanopore TiO_2 (anatase, size: 15−30 nm) is about $10^{-4}-10^{-6}$ $cm^2/(V\ s)$ and depends on the inhomogeneous interparticle transport barriers.[52] For ZnTCPP/TiO_2 systems, after photoexcitation, ZnTCPP* injects an electron into the conduction band or into the energetically accessible surface states of the semiconductor driven by the energy difference (ΔE) between the lowest unoccupied molecular orbital (LUMO) of ZnTCPP (3.4 ± 0.2 eV) and the conduction band of TiO_2 (4.4 ± 0.2 eV).[53] In our experiment as well as in other published work,[7,8,54] there is no external circuit implicated in the experiment as we focus on the fundamental interfacial electron transfer dynamics and not on a specific technical development of a solar cell; therefore, the cation cannot be compensated after the FET, and the electron diffusion will be affected by the Onsager distance (Rc) because

(45) Pan, D.; Hu, D.; Lu, H. P. *J. Phys. Chem. B* **2005**, *109*, 16390–16395.
(46) Lu, H. P.; Xun, L.; Xie, X. S. *Science* **1998**, *282*, 1877–1882.
(47) Mihailetchi, V. D.; Koster, L. J. A.; Hummelen, J. C.; Blom, P. W. M. *Phys. Rev. Lett.* **2004**, *93*, 216601 (1−4).
(48) Morteani, A. C.; Sreearunothai, P.; Herz, L. M.; Friend, R. H.; Silva, C. *Phys. Rev. Lett.* **2004**, *92*, 247402 (1−4).
(49) Onsager, L. *Phys. Rev.* **1938**, *54*, 554–557.
(50) Braun, C. L. *J. Chem. Phys.* **1984**, *80*, 4157–4161.
(51) Marsh, R. A.; McNeill, C. R.; Abrusci, A.; Campbell, A. R.; Friend, R. H. *Nano Lett.* **2008**, *8*, 1393–1398.
(52) Dittrich, T.; Lebedev, E. A.; Weidmann, J. *Phys. Status Solidi A* **1998**, *165*, R5−R6.
(53) Wienke, J.; Schaafsma, T. J.; Goossens, A. *J. Phys. Chem. B* **1999**, *103*, 2702–2708.
(54) Weng, Y. X.; Wang, Y. Q.; Asbury, J. B.; Ghosh, H. N.; Lian, T. Q. *J. Phys. Chem. B* **2000**, *104*, 93–104.

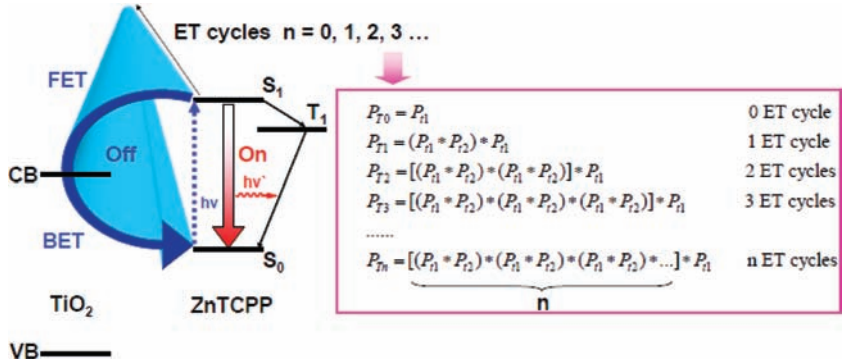

Figure 3. Schematic presentation of energy levels, basic photoinduced process, and convoluted multiple ET cycles in ZnTCPP/TiO_2 system. Probability distributions of photon-to-photon pair times P_{Tn} are expressed as the convolution of the probability of laser waiting time P_{t1} and probability of BET time P_{t2}.

of the mutual Coulombic attraction force of the geminate electron−cation pair, e^-/$ZnTCPP^+$. The Onsager distance in anatase TiO_2 is about 11−18 Å (according to reported dielectric constant from 31 to 50).[55−57] At the Onsager distance, there is a 50% probability that a geminate pair of electron and cation escapes from a recombination. Previous Stark effect spectroscopy studies[58] suggested that the FET injection distance, d_e, is averagely much shorter than 10 Å, which is therefore shorter than the Onsager distance. Driven by the Coulombic field, the excess electron comes back and recombines with the parent cation in the cycles of the single-molecule interfacial electron transfer process. For the TiO_2 nanoparticles used in our experiments, the possible free-electron density is extremely low,[59] and the electron−cation recombination is geminate between the excess electron and the parent cation of e^-/$ZnTCPP^+$.

We have demonstrated that detected signal photons are emitted from nanosecond transition from $S_1 \rightarrow S_0$ of ZnTCPP[4,37] except rare photons from background and phosphorescence; phosphorescence efficiency is lower than 10^{-4} at room temperature.[60] Within a photon-to-photon pair time, two types of events occur: (1) fluorescence excitation and emission that are intrinsically stochastic processes giving no correlation among the pair times, as evident in Figure 2 which shows no autocorrelation for the pair times of ZnTCPP on a glass surface, and (2) interfacial electron transfer which involves both FET and BET. FET typically occurs in fs to ps time scales, whereas BET occurs in subns to ms time scales. Consequently, the photon-to-photon pair time at μs−ms time scale is dominated by BET time and the excitation-photon waiting time at the μs time scale. Furthermore, with the ET reactivity fluctuating from time to time, the ET process may continuously involve multiple FET−BET cycles before giving out a photon (as shown in Figure 3). Therefore, for the pair times involving the ET process, they include convoluted multiple Poisson events, and the convoluted multiple Poisson rate processes give rise to the correlation of the photon-to-photon pair times.

We have conducted a theoretical simulation and analysis based on the above single-molecule interfacial recombination ET model (Figure 3). The excitation-photon waiting time, t_1, is intrinsically stochastic and is defined as an exponential rate process: $P_{t1} = A_1 \exp(-t_1/\tau_1)$, where P_{t1} is the probability of the t_1, and τ_1 is the mean of the distribution. From the distribution of the pair times of a bright state (Figure 2), τ_1 is deduced to be ~0.32 ms for this molecule. The BET rate process, because of its complexity, has been reported to be single exponential,[61−63] multiexponential,[22,26,54,64−71] or stretched exponential.[7,22,24,72−77] Here, on the basis of the recombination model, the coulomb force between the electron and the cation across the interface dominates the diffusional drift of the electron typically involving trapping and detrapping in the semiconductor bulk and surface. It is reasonable to assume that the BET time will mostly be determined by the initial electron ejection depth into a TiO_2 nanoparticle, however, d_e is determined by the

(55) Tang, H.; Prasad, K.; Sanjinès, R.; Schmid, P. E.; Lévy, F. *J. Appl. Phys.* **1994**, *75*, 2042–2047.
(56) Oja, I.; Mere, A.; Krunks, M.; Nisumaa, R.; Solterbeck, C. H.; Es-Souni, M. *Thin Solid Films* **2006**, *515*, 674–677.
(57) Goossens, A.; van der Zanden, B.; Schoonman, J. *Chem. Phys. Lett.* **2000**, *331*, 1–6.
(58) Walters, K. A.; Gaal, D. A.; Hupp, J. T. *J. Phys. Chem. B* **2002**, *106*, 5139–5142.
(59) For ZnTCPP spin-coated TiO_2 (anatase) surface, without photoexcitation, the free-electron density inside TiO_2 is demonstrated to be 2×10^{16} cm^{-3}.[41] Taking TiO_2 nanoparticle as a sphere with diameter of 15 nm, the amount of free electrons inside one TiO_2 nanoparticle is deduced to be 0.035.
(60) Kalyanasundaram, K.; Neumannspallart, M. *J. Phys. Chem.* **1982**, *86*, 5163–5169.
(61) Martini, I.; Hodak, J. H.; Hartland, G. V. *J. Phys. Chem. B* **1999**, *103*, 9104–9111.
(62) Martini, I.; Hodak, J. H.; Hartland, G. V. *J. Phys. Chem. B* **1998**, *102*, 9508–9517.
(63) Martini, I.; Hodak, J.; Hartland, G. V.; Kamat, P. V. *J. Chem. Phys.* **1997**, *107*, 8064–8072.
(64) Vrachnou, E.; Vlachopoulos, N.; Grätzel, M. *J. Chem. Soc., Chem. Commun.* **1987**, 868–870.
(65) Lu, H.; Prieskorn, J. N.; Hupp, J. T. *J. Am. Chem. Soc.* **1993**, *115*, 4927–4928.
(66) Ghosh, H. N.; Asbury, J. B.; Weng, Y. X.; Lian, T. Q. *J. Phys. Chem. B* **1998**, *102*, 10208–10215.
(67) Ellingson, R. J.; Asbury, J. B.; Ferrere, S.; Ghosh, H. N.; Sprague, J. R.; Lian, T. Q.; Nozik, A. J. *J. Phys. Chem. B* **1998**, *102*, 6455–6458.
(68) Hilgendorff, M.; Sundström, V. *J. Phys. Chem. B* **1998**, *102*, 10505–10514.
(69) Haque, S. A.; Tachibana, Y.; Klug, D. R.; Durrant, J. R. *J. Phys. Chem. B* **1998**, *102*, 1745–1749.
(70) Asbury, J. B.; Ellingson, R. J.; Ghosh, H. N.; Ferrere, S.; Nozik, A. J.; Lian, T. Q. *J. Phys. Chem. B* **1999**, *103*, 3110–3119.
(71) Ramakrishna, G.; Ghosh, H. N. *J. Phys. Chem. B* **2001**, *105*, 7000–7008.
(72) Nelson, J. *Phys. Rev. B* **1999**, *59*, 15374–15380.
(73) Nelson, J.; Chandler, R. E. *Coord. Chem. Rev.* **2004**, *248*, 1181–1194.
(74) Nelson, J.; Haque, S. A.; Klug, D. R.; Durrant, J. R. *Phys. Rev. B* **2001**, *63,* 205321 (1−9).
(75) Trachibana, Y.; Haque, S. A.; Mercer, I. P.; Durrant, J. R.; Klug, D. R. *J. Phys. Chem. B* **2000**, *104*, 1198–1205.
(76) Benkö, G.; Hilgendorff, M.; Yartsev, A. P.; Sundström, V. *J. Phys. Chem. B* **2001**, *105*, 967–974.
(77) Huber, R.; Sporlein, S.; Moser, J. E.; Grätzel, M.; Wachtveitl, J. *J. Phys. Chem. B* **2000**, *104*, 8995–9003.

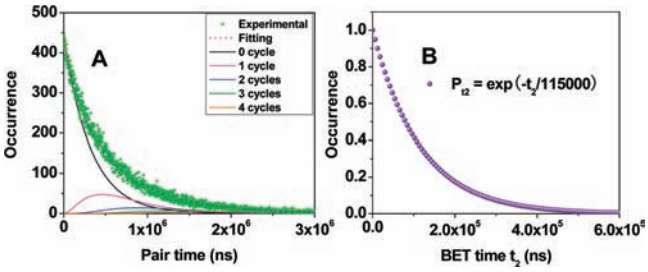

Figure 4. Fitting results of the colored state in trajectory of Figure 2. (A) Histogram of pair times and the fitted exponential and nonexponential processes by convoluting multiple ET involved events (cycles ranging from zero to four). (B) Normalized distribution of BET times.

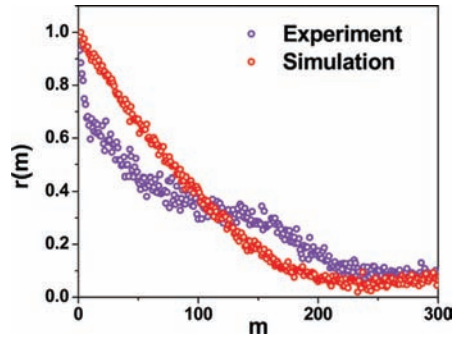

Figure 5. Normalized autocorrelation functions of the experimental and simulated photon pair times for ET-active state in Figure 2.

stochastic fluctuation of the interfacial electronic coupling between ZnTCPP and the TiO_2 nanoparticle. Therefore, to simplify the fitting and simulation analysis, we take the BET time t_2 distribution as a single Poisson distribution, $P_{t2} = A_2 \exp(-t_2/\tau_2)$, where P_{t2} is the probability of the t_2, and τ_2 is the mean of the distribution.

Because the convolution of the excitation-photon waiting time t_1 and of the the BET time t_2 dominates the duration of an ET cycle, the probability distribution of photon-to-photon pair time P_{Tn} (Tn is the pair time, and n is the number of ET cycles) can be described as the convolution of P_{t1} and P_{t2} as shown in Figure 3. Function P_{Tn} can be directly calculated by integral calculus. For example, the probability distribution for one-cycle ET pair times is expressed as

$$P_{T1} = A_1^2 A_2[(kt - 1)e^{-k_1 t} + e^{-k_2 t}]/k^2$$

where $k_1 = 1/\tau_1$, $k_2 = 1/\tau_2$, $k = k_2 - k_1$, and t is the real photon-to-photon pair time. In our data analysis, we performed programmable convolution and fitting using Matlab (R2007a). Parameters τ_2 and n can be directly obtained. According to the convoluted single-molecule ET dynamics, we analyzed the histograms of the single-molecule pair time trajectories. Figure 4 shows a fit result analyzing a portion (shown in color) of a single-molecule fluorescence trajectory (Figure 2). Our data analysis shows that the histograms of the pair times can be fitted well by assuming that there is a maximum of four ET cycles during a photon-to-photon pair time (Figure 4A). Our fitting result shows that the histograms of pair times of the zero cycles are exponential distributions whereas the histograms of pair times involved in ET cycles are nonexponential distributions. By calculating the probabilities from the histograms, we demonstrate that the excited states have a 36% probability to be involved in electron-transfer events and that the percentages of reactions involving one to four ET cycles are 20%, 8%, 4.5%, and 2.9%, respectively. In most of the ET events, the excited state performs one ET cycle ($S_0 + h\nu_{excitation} \rightarrow S_1 \rightarrow$ FET&BET $\rightarrow S_0$) and then emits one emission photon ($S_0 + h\nu_{excitation} \rightarrow S_1 \rightarrow S_0 + h\nu_{emission}$). Moreover, an average BET time, τ_2, is fitted to be about 120 ± 10 μs by calculating the mean of the distribution of BET times (Figure 4B). Considering that not every emitted photon is detected and that a typical detection efficiency for a single-molecule imaging microscope is about 10% (i.e., only 1 out of 10 photons is detected[46]), we suggest that the actual single-molecule BET rate process probed is at 10^{-5} s. This value is consistent with the widely reported BET times ranging from subns to several ms for dye/semiconductor systems.[7,8,14,18,22,24,26]

To further analyze the single-molecule interfacial ET dynamics, we have simulated photon-to-photon pair times from zero ET cycle to four ET cycles initiated by consecutive laser photon excitation events. Because of single-molecule interfacial ET reactivity fluctuations, the experimentally detected photon-to-photon pair times in a single-molecule fluorescence trajectory are a mixture of pair times originated from radiative emission, ET events with different cycles, and background noise. To simulate the trajectory of pair times, random numbers are first generated on the basis of the fitted exponential and nonexponential curves in Figure 4. Random numbers that originated from the exponential curve are the analogue of pair times only from radiative emission (zero ET cycle). Random numbers that originated from the nonexponential curves are the analogue of pair times from ET events with different cycles (one to four). After 10% noise is randomly dispersed in the above generated pair times, a simulated trajectory of pair times is generated by programming control according to their occurring possibilities (Figure 4). Figure 5 shows the experimental and simulated autocorrelation function of pair times, where the experimental autocorrelation function is calculated from the same data shown in Figure 2 (the colored portion of the emission trajectory) and Figure 4. Although only the primary components of the experimental and simulated autocorrelation functions show the similar decay behavior, as the experimental autocorrelation function contains more measurement noise, the simulated autocorrelation function essentially presents the experimental autocorrelation primary components which disappear at the index of 250 (Figure 5).

The interfacial electron transfer reactivity is highly sensitive to the molecular interactions between the adsorbed dye molecules and the TiO_2 substrate. There are a few parameters that contribute to the molecular interactions and in turn regulate the ET reactivity fluctuations; the parameters include (1) the driving force of free-energy gap, (2) the vibrational relaxation energy of the adsorbed molecules and the surface vibrational modes of TiO_2, (3) and the electronic coupling between the dye and the TiO_2.[4,24,78−80] Among these parameters, the electronic coupling and surface bonding likely provide the most significant contributions to the interfacial electron transfer rate fluctuations. For the ZnTCPP/TiO_2 ET system, the correlation of the photon-to-photon pair times of an ET-active state is interpreted by the interfacial electron−cation recombination model including the interfacial ET reactivity fluctuation at an ms time scale. In previous reports by us and others, interfacial ET transfer reactivity has been demonstrated as intermittent and as fluctuat-

(78) Pan, D.; Hu, D.; Lu, H. P. *J. Phys. Chem. B* **2005**, *109*, 16390–16395.
(79) Yan, S. G.; Hupp, J. T. *J. Phys. Chem.* **1996**, *100*, 6867–6870.
(80) Watson, D. F.; Marton, A.; Stux, A. M.; Meyer, G. J. *J. Phys. Chem. B* **2004**, *108*, 11680–11688.

ing from time to time at a single-molecule level.[4,36−38] Though the interfacial ET dynamics are complex and inhomogeneous in nature, the approach presented here is demonstrated to be effective in probing the real-time ET picture and in getting BET time.

In conclusion, we have probed and analyzed the single-molecule interfacial electron−cation recombination dynamics at a precise photon-to-photon pair time scale of subms to μs time scales by single-molecule photostamping spectroscopy. The autocorrelated photon-to-photon pair time of an ET-active state, which conceals the real-time characteristics of the interfacial electron−cation recombination dynamics, has been revealed and applied to probe the BET dynamics of ZnTCPP/TiO_2 system. On the basis of a convoluted interfacial electron−cation recombination model, the BET time is deduced to be on a 10^{-5} s time scale, which is consistent with the ensemble-averaged measurements which demonstrate the BET time ranging from subnanosecond to millisecond time scale. The autocorrelation of photon-to-photon pair times as well as the convoluted ET model has been further demonstrated by simulation and has been interpreted in terms of the interfacial ET reactivity fluctuation and blinking. Our approach not only can effectively probe the single-molecule interfacial electron−cation dynamics but also can be applied to other single-molecule ground-state regeneration dynamics at interfaces and in condensed phases.

Acknowledgment. H. P. L. acknowledges the support of our research from the Office of Basic Energy Sciences within the Office of Science of the U. S. Department of Energy (DOE)(Grant DE-FG02-06ER15827) and from the Chemistry Division of the National Science Foundation (NSF) (Grant 0822694).

JA902640Q